NATIONAL AERONAUTICS AND SPACE ADMINISTRATION

Ranger VIII
Photographs of the Moon

PHOTOGRAPHIC EDITION

JET PROPULSION LABORATORY
CALIFORNIA INSTITUTE OF TECHNOLOGY
December 15, 1965

NATIONAL AERONAUTICS AND SPACE ADMINISTRATION

Ranger VIII
Photographs of the Moon

PHOTOGRAPHIC EDITION

JET PROPULSION LABORATORY
CALIFORNIA INSTITUTE OF TECHNOLOGY
December 15, 1965

Jet Propulsion Laboratory
California Institute of Technology

Prepared under Contract No. NAS 7-100
National Aeronautics and Space Administration

Ranger VIII Photographs of the Moon

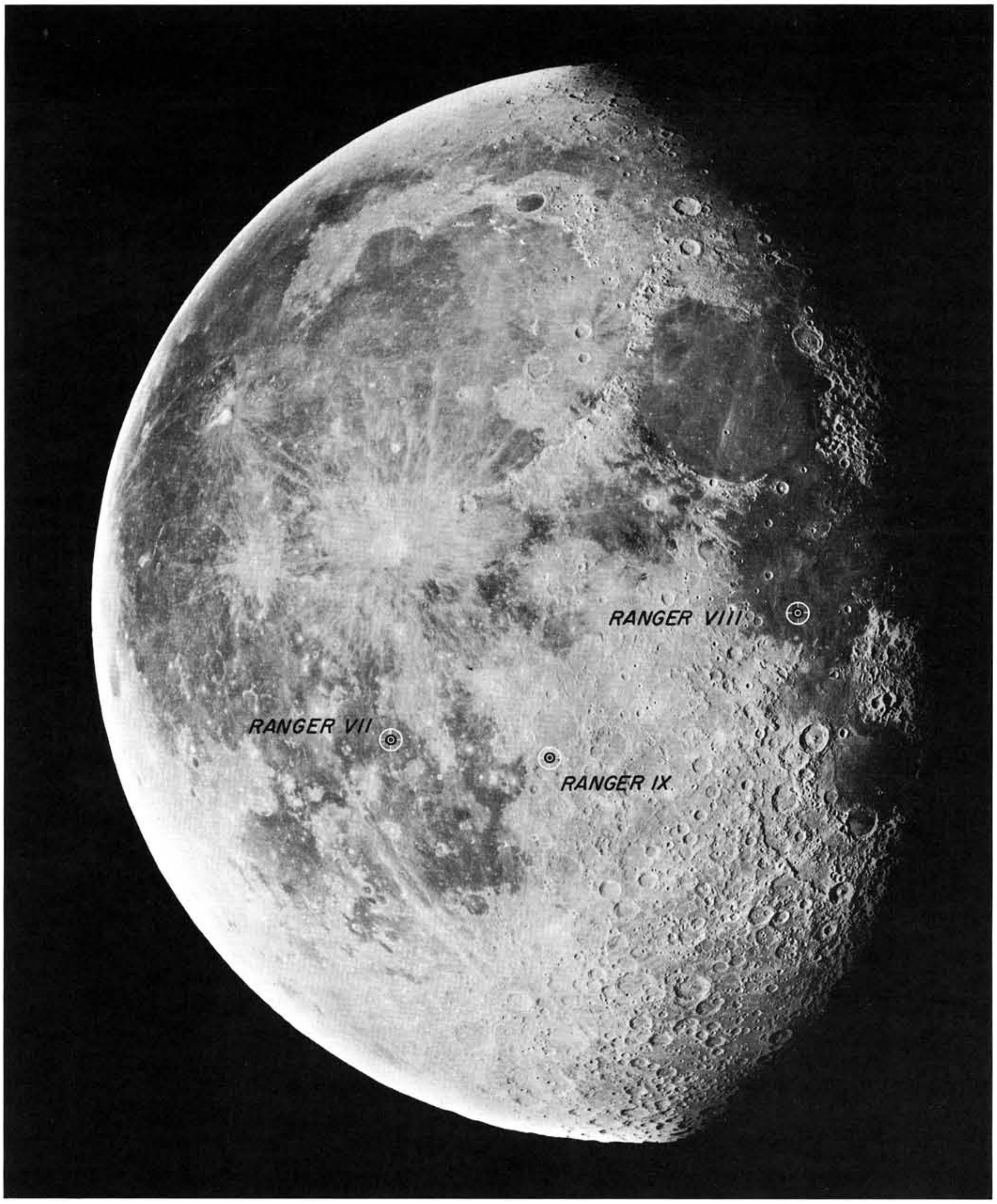

Ranger impact points*

*Lick Observatory photograph

FOREWORD

This volume of *Ranger VIII* photographs of the Moon is the fourth of five volumes presenting the photographs of the Moon taken by *Ranger VII**, *VIII,* and *IX. Ranger VIII* impacted the Moon on February 20, 1965, less than 20 km from the selected impact point in Mare Tranquillitatis. The frontispiece shows the impact points of all three successful *Ranger* spacecraft on a telescopic photograph of the Moon, taken with the terminator at 39°East as it was at the time of the *Ranger VIII* impact.

During the 23 min the cameras operated before impact, a large swath of Moon was photographed for the first time at high resolution. The early, lower-resolution pictures were taken of areas far from the terminator, where the lighting conditions were poor. As the spacecraft approached the surface, the cameras traced diagonally across the continental region between Mare Nubium and Mare Tranquillitatis. Excellent photographs of Delambre, the southern shoreline of Tranquillitatis, and the crater pair Ritter and Sabine were obtained. The final minutes before impact yielded high-resolution photographs of Mare Tranquillitatis which satisfied the prime objective of *Ranger VIII*. The difference in viewing direction between the A and B cameras, in conjunction with the spacecraft attitude, provided a feature unique to the *Ranger VIII* pictures: the convergence between the two cameras can be used to construct stereometric models for the derivation of elevation information over much of the total area covered.

The photographs for this volume have been selected on the basis of a careful evaluation of the area coverage, resolution, and overlap of the pictures**. A selection of 60 from the 270 A-camera photographs was made as follows:

1. Five frames at a scale increase of about 33% from the first 190 frames.
2. Five frames at a 10% scale change from the next 30 frames.
3. All of the last 50 frames.

**Ranger VII, Photographs of the Moon, Part I: Camera "A" Series,* August 27, 1964; *Part II: Camera "B" Series,* December 15, 1964; *Part III: Camera "P" Series,* February 10, 1965.

**Selection of the photographs was made by E. A. Whitaker of the University of Arizona, the negatives were processed by R. Wichelman of JPL, and the photographic printing was done by Ray Manley, Commercial Photography, Inc., Tucson, Arizona.

A total of 20 B-camera frames were chosen in the following way:

1. Forty frames at a scale difference of about 10% from the first 220 frames.
2. All of the last 50.

The selection of frames from the P cameras was limited to the final 15 high-resolution pictures, plus five others chosen for particular features shown in them. The remaining P frames were not used because of the overlapping coverage of the A and B cameras.

This set of volumes is being prepared in order to provide the scientific community with the results of the *Ranger* missions. The efforts of the *Ranger* Experimenter team have led to the publication of the results of the *Ranger VII* mission†, which will soon be followed by a report on the *Ranger VIII* and *IX* missions††. The *Ranger* Experimenter team which has been conducting the initial scientific evaluation has as its members the following scientists:

Principal Investigator	Dr. Gerard P. Kuiper, Director, Lunar and Planetary Laboratory, University of Arizona, Tucson, Arizona.
Co-experimenters	Mr. R. L. Heacock, Chief, Lunar and Planetary Instruments Section, Jet Propulsion Laboratory, Pasadena, California.
	Dr. E. M. Shoemaker, Chief, Astrogeology Branch, U.S. Geological Survey, Flagstaff, Arizona.
	Dr. H. C. Urey, Professor at Large, School of Science and Engineering, University of California at La Jolla, California.
	Mr. E. A. Whitaker, Research Associate, Lunar and Planetary Laboratory, University of Arizona, Tucson, Arizona.

†*Ranger VII, Part II: Experimenters' Analyses and Interpretations,* Technical Report No. 32-700, February 10, 1965.

††*Ranger VIII and IX, Part II: Experimenters' Analyses and Interpretations,* Technical Report No. 32-800 (to be published).

CONTENTS

I. Introduction . . . 1

II. *Ranger VIII* Mission Description and Trajectory . . . 2

III. Impact-Area Selection and Camera Terminal Alignment . . . 6

IV. Television System Description . . . 7
- A. Cameras . . . 7
- B. Receiving and Recording Equipment . . . 7
- C. Camera Calibration . . . 8
- D. Film Processing . . . 9

V. Camera Tables of Values . . . 11

References . . . 17

TABLES

1. Camera characteristics . . . 7
2. *Ranger VIII* preliminary tables of values . . . 13

FIGURES

1. Lunar encounter geometry . . . 3
2. Spacecraft coordinate system . . . 4
3. *Ranger VIII* camera fields of view . . . 5
   - (a) Cameras A and B . . . 5
   - (b) Cameras P_1 and P_2 . . . 6
   - (c) Cameras P_3 and P_4 . . . 6
4. Typical light-transfer characteristics . . . 8
5. Typical sine-wave response . . . 9
6. *Ranger VIII* area coverage . . . 10
7. Definition of central reticle, deviation north, and scale . . . 11
8. Altitude and definition . . . 12
9. *Ranger VIII* photometric geometry . . . 12

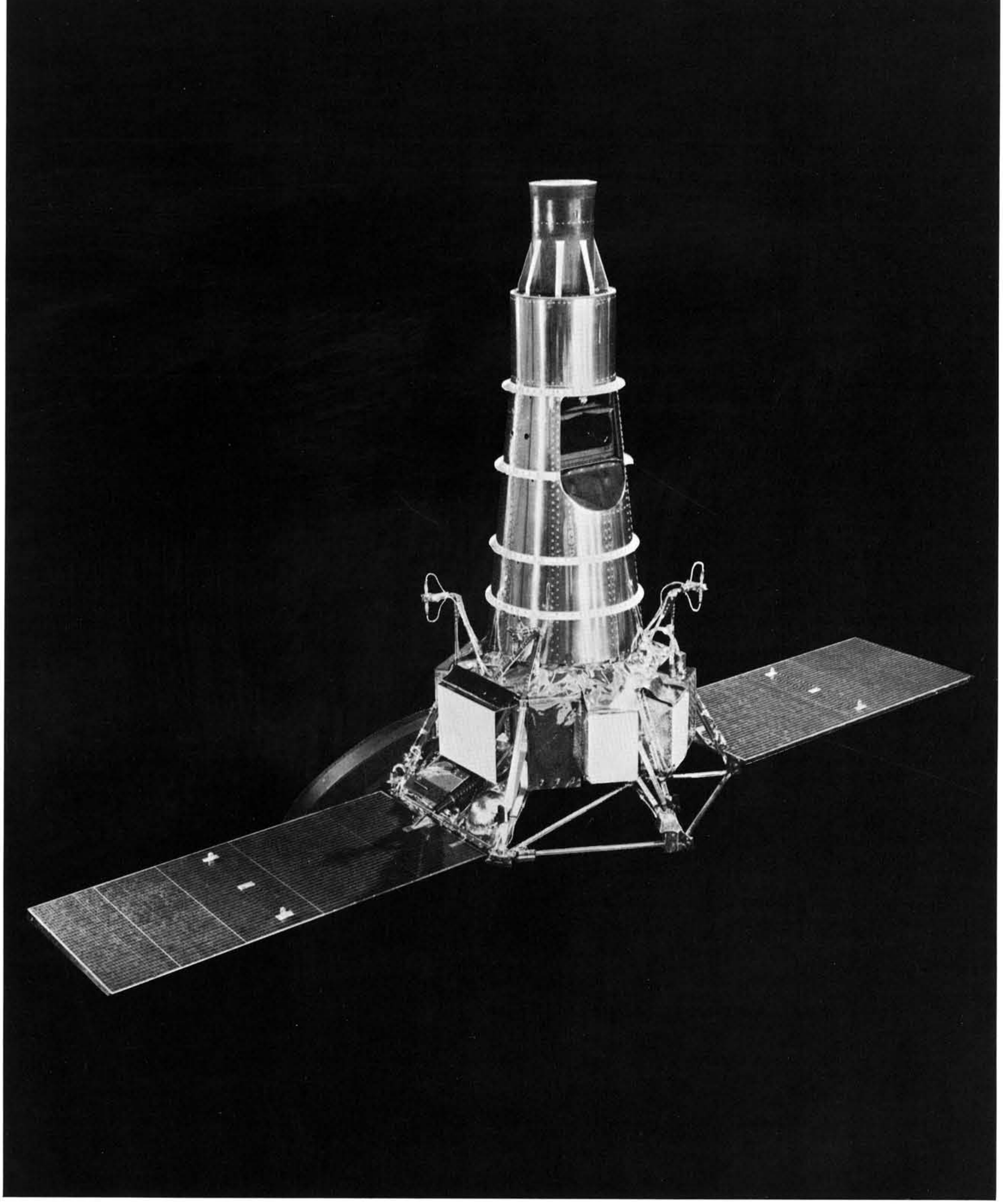

I. INTRODUCTION*

The development of the basic *Ranger* spacecraft system was initiated in 1959. The spacecraft was conceived as a fully attitude-stabilized platform from which lunar or planetary observations could be made by mounting alternate payloads on top of the basic spacecraft. A new concept involving a parking orbit was also proposed in order to permit maximum payloads to be injected on the most efficient lunar or planetary trajectory. The technique involves two burns of the second stage of the *Atlas/Agena B* launch vehicle to compensate for the nonideal geographical location of the launch pad and provide a more practical daily launch window.

The advantages to be gained from an attitude-stabilized spacecraft configuration include:

1. Maximum effectiveness in generating power by accurately pointing solar panels at the Sun.
2. Establishment of an accurate angle-reference system for use as a coordinate system in which to perform a midcourse maneuver to trim the flight path and as a reference for terminal orientation.
3. Provision of maximum communications by accurately pointing a high-gain antenna at the Earth.
4. Feasibility of using scientific instruments which require direction determination and/or control to make their observations.

The nominal sequence of spacecraft operation after separation from the *Agena B* involves extending the solar panels and pointing the roll axis at the Sun for maximum solar power. The attitude-control system uses inputs from optical sensors to control small cold-gas jets to obtain and maintain proper attitude orientation. When the spacecraft is sufficiently far from the Earth, the antenna hinge angle is nominally set to point the optical Earth sensor and the high-gain antenna at the Earth. The control jets roll the spacecraft until the optical Earth sensor locks onto the Earth and high-gain directional communication is made possible. Establishing Sun and Earth orientation in this manner provides full attitude stabilization for the cruise mode.

The midcourse maneuver is performed by establishing an appropriate pointing direction relative to the Sun–spacecraft–Earth coordinate system and firing a midcourse rocket engine to obtain the desired velocity increment. A radio-command system transmits the angles and velocity-increment requirements to the spacecraft. The commands are stored and acted upon in a controlled sequence using a gyro-stabilized reference system to achieve the required orientation. Once the midcourse maneuver is complete, the spacecraft automatically resumes the cruise-mode orientation.

The spacecraft has the ability to perform a limited angular orientation in a terminal-maneuver sequence if required. The principal constraint upon orientation geometry involves maintaining the high-gain antenna pointed at the Earth.

The *Ranger* Block III project (consisting of *Ranger VI* through *IX*) was initiated in mid-1961. The objective of high-resolution photographs of the lunar surface could conceptually be achieved through any of several approaches, ranging from systems using long focal-length optics to a technique involving a retro-firing sequence. The approach which was selected used more conventional techniques and available technology. A high-power transmitter was used to provide sufficient video bandwidth for a rapid framing sequence of television pictures to impact. Two separate channels were proposed for redundancy and to permit both narrow- and wide-angle camera coverage.

The camera fields of view were arranged to provide overlapping coverage so that, with a nominal terminal orientation, a nesting sequence of photographs would be obtained from at least one of the wide-angle cameras. The narrow-angle camera frame sequence is over ten times faster than the wide-angle camera sequence to permit operation closer to the surface for higher resolution. The final design of the system included two cameras in the wide-angle system and four cameras in the narrow-angle system.

*The sections that follow were prepared by Gerald M. Smith, Donald E. Willingham, and William E. Kirhofer of the Jet Propulsion Laboratory, California Institute of Technology.

II. RANGER VIII MISSION DESCRIPTION AND TRAJECTORY

Ranger VIII was launched from Cape Kennedy on February 17, 1965, at 17:05:01 GMT, after a very smooth countdown with no unscheduled holds. The launch resulted in a trajectory which would pass close to the trailing edge of the Moon. The necessary midcourse maneuver was then calculated and executed to guide the spacecraft to the desired target area. During the launch, all booster-vehicle and spacecraft events occurred as planned. The initial *Atlas D/Agena B* boost placed the *Agena* and spacecraft in a parking orbit over the Atlantic Ocean, where the *Agena* second burn was initiated. Termination of this final boost phase accomplished the injection of the spacecraft into an Earth–Moon transfer orbit. After separation from the *Agena*, the spacecraft solar panels were extended and Sun and Earth acquisition were accomplished in a normal manner.

Telemetry and doppler velocity data received during the midcourse-motor burn confirmed the desired midcourse correction. The spacecraft then returned to cruise mode by reacquiring the Sun and Earth. Post-midcourse tracking data indicated that the spacecraft would impact the Moon in the selected target area, 3°North and 24°East selenocentric coordinates.

After the midcourse maneuver, the terminal approach was analyzed considering the angle of illumination of the lunar surface, the direction of the velocity vector of the spacecraft, and the pointing direction of the camera system. It was established that no terminal maneuver was required for the photographic sequence. The wide-angle camera system started taking pictures at 09:34:33 GMT on February 20, 1965, 23 min, 4 sec prior to impact. The narrow-angle system initiated transmission of pictures at 09:34:27 GMT, 23 min, 10 sec prior to impact. Both camera systems operated to impact at 09:57:37 GMT. The last narrow-angle picture was taken 0.09 sec before impact from an altitude of approximately 160 meters. The resolution in the final frames was limited by image motion to about 1.1 meters.

The spacecraft encountered the Moon in direct motion along a hyperbolic trajectory, with incoming asymptote direction at an angle of −13.6° from the lunar equator. The orbit plane was inclined 16.5° to the lunar equator. Thus, the subspacecraft trace on the lunar surface was initially below the lunar equator by approximately 13° and proceeded in a northeasterly direction, crossing the equator at a selenocentric east longitude of 15.3° in a direction 16.1° north of east 3 min prior to impact.

At the time of the first wide-angle picture, the spacecraft selenocentric south latitude and west longitude were 7.3 and 10.9°, respectively. At impact, the velocity vector was 48.4° from the local vertical in a direction, projected into the local horizon, 74.1° east of north. The velocity of the spacecraft at impact was 2.653 km/sec. The encounter geometry illustrated in Fig. 1 relates the trajectory and lunar trace with the lunar area viewed by each wide-angle camera. In addition, Fig. 1 gives the trace on the lunar surface viewed by the optical axis of the wide-angle cameras prior to lunar impact.

During the cruise mode and terminal portion of flight, the *Ranger VIII* spacecraft was stabilized by a cold-gas jet attitude-control system. This system derived its reference from the Sun and Earth. The Sun sensors allowed the spacecraft roll axis to be aligned with the $-Z$ axis toward the Sun. The Earth sensor was used to orient the high-gain antenna toward Earth. This orientation kept the Earth in the $-Y,Z$ plane of the spacecraft. The X,Y, and Z orthogonal coordinate system associated with the spacecraft is defined in Fig. 2.

The reference direction for the camera alignment was 38° from the Z (or roll) spacecraft axis. The optical centers of all the cameras were within 0.5° of the spacecraft Y,Z plane. The relative camera alignment with spacecraft coordinates is shown in Fig. 3.

At lunar encounter, the Moon was within 3 days of its third quarter, with the projection of the Sun at a selenocentric south latitude and west longitude of 1.5 and 50.5°, respectively. The lunar libration was such that the projection of the Earth was at a lunar south latitude of 51° and east longitude of 6.9°. Thus, with the Sun and Earth as reference, the Y,Z spacecraft plane was then inclined to the lunar equator by approximately 5°. Because the camera axes are nearly contained in the Y,Z spacecraft plane, the cameras were, in general, pointing north of the lunar equatorial plane by approximately 5°.

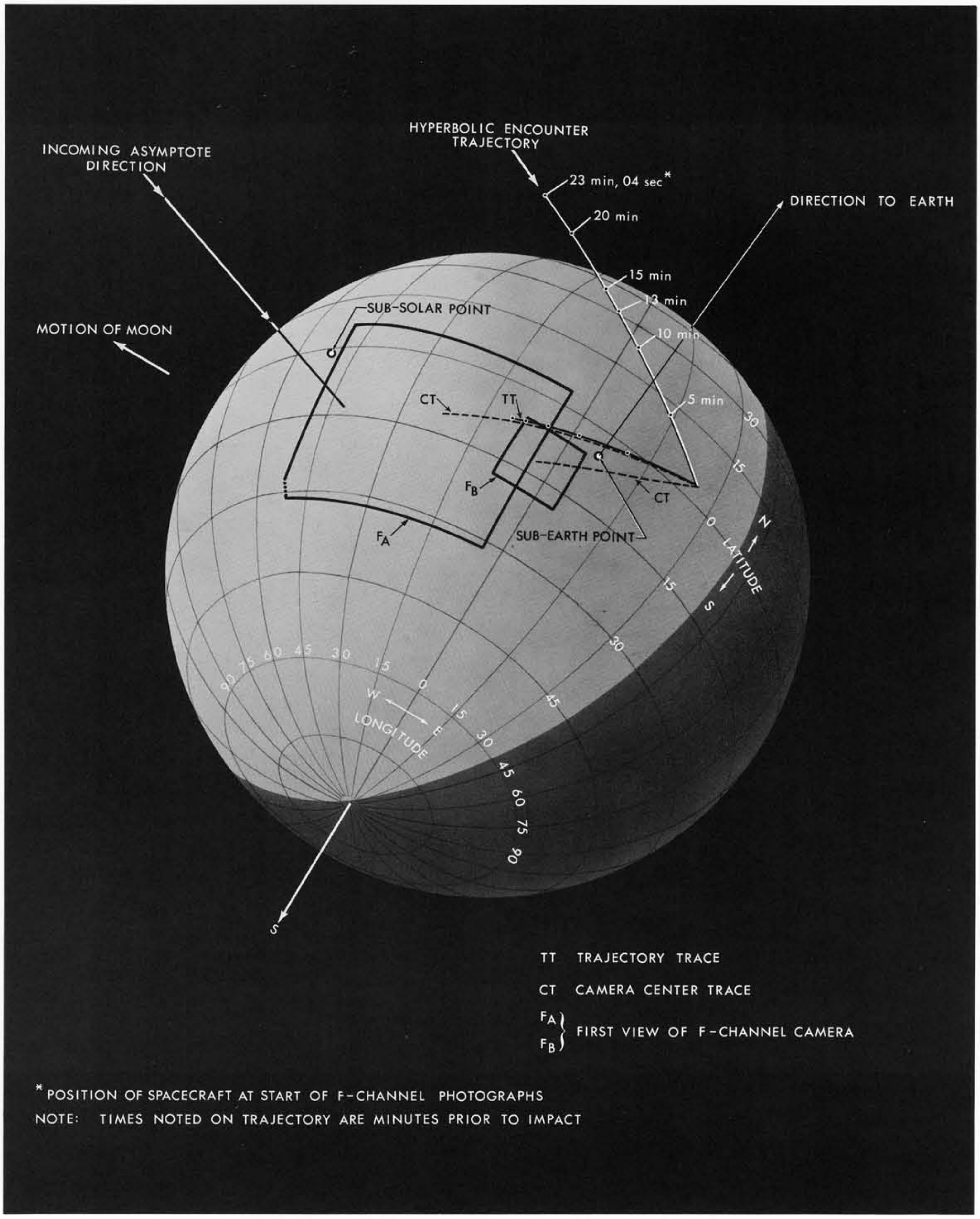

Fig. 1. Lunar encounter geometry

Fig. 2. Spacecraft coordinate system

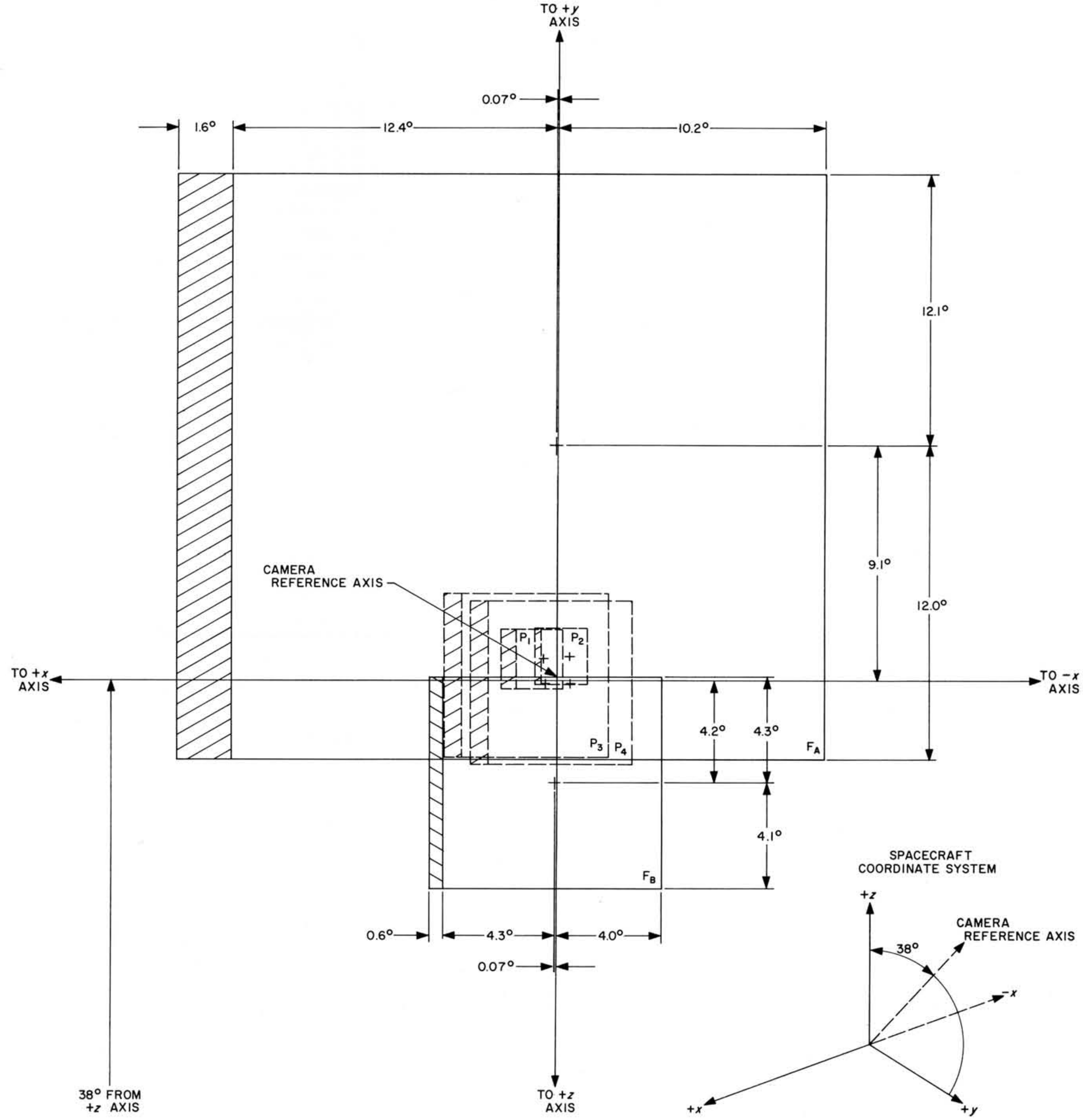

Fig. 3. *Ranger VIII* **camera fields of view (a) Cameras A and B**

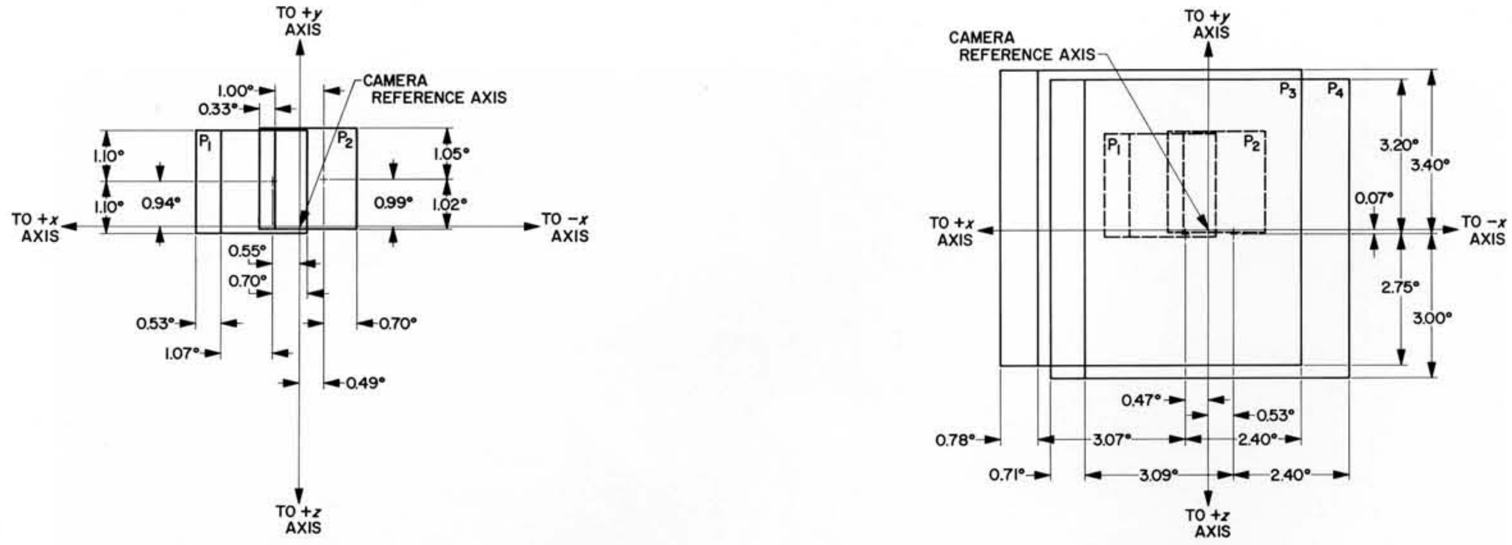

(b) Cameras P_1 and P_2

(c) Cameras P_3 and P_4

Fig. 3. (cont'd)

III. IMPACT-AREA SELECTION AND CAMERA TERMINAL ALIGNMENT

The basic objective in selecting the *Ranger VIII* target was to choose an area which, in conjunction with the *Ranger VII* photographs, would be most useful in increasing the knowledge of the lunar maria. Since *Ranger VII* had photographed a brownish mare overlaid with weak rays from Copernicus and Tycho, it was considered that a dark, ray-free mare area would best complement the existing data and permit reasonable extrapolations to be made to other mare areas not photographed at high resolution. Such an area—Mare Tranquillitatis—was available to *Ranger VIII* on the first day of the launch period, February 17, 1965. Taking into consideration *Apollo* constraints, as well as the guidance performance of *Ranger VI* and *VII*, a point near the equator and 15° from the terminator was chosen. The coordinates of this point were 24°East longitude and 3°North latitude.

As was the case with *Ranger VII*, the spacecraft remained in cruise-mode orientation for the picture-taking sequence; however, the reasons for which this orientation was decided on were different (see Fig. 6). As the spacecraft descended to impact, the B camera would lead the wider-angle A camera; because of the sharp descent, this arrangement would provide a maximum in stereo coverage, thus facilitating the interpretation of the lunar relief recorded by the pictures. In addition, relatively high-resolution photographs would be obtained of the highland region bounding Mare Tranquillitatis. The cruise-mode orientation also maximized the area coverage. On the basis of these considerations, it was recommended that no change be made in camera orientation even though the last frames would be blur-limited.

The final B frame covers an area 2.1 × 1.5 km, with an approximate resolution of 2.6 meters. The P_3-camera picture was the only one in the last P frame not seriously degraded by the image motion. Its resolution, however, is about the same as the image-motion magnitude, i.e., 1.1 meter.

IV. TELEVISION SYSTEM DESCRIPTION

A. Cameras

The *Ranger* Block III spacecraft television system contains six cameras, divided into two separate channels designated P and F. Each channel is self-contained, with separate power supplies, timers, and transmitters. All six cameras are fundamentally the same, with differences in exposure times, fields of view, lenses, and scan rates distinguishing the individual cameras (Table 1).

Table 1. Camera characteristics

Characteristic	Camera					
	A	B	P_1	P_2	P_3	P_4
Focal length, mm	25	76	76	76	25	25
f number	1.0	2.0	2.0	2.0	1.0	1.0
Frame time, sec	2.56	2.56	0.2	0.2	0.2	0.2
Horizontal frequency, cps	450	450	1500	1500	1500	1500
Exposure time, msec	5	5	2	2	2	2
Field of view*, deg	25	8.4	2.1	2.1	6.3	6.3
Target size, deg	11	11	2.8	2.8	2.8	2.8
Scan lines	1150	1150	300	300	300	300
Time between frames, sec	5.12	5.12	0.84	0.84	0.84	0.84

*The actual field of view is somewhat smaller than the given numbers because of the presence of a mask at the edge of the vidicon target which is used to determine scene black on each scan of the electron beam.

One-inch-diameter vidicons are used for image sensing. Electromagnetically driven slit-type shutters expose the vidicons. The image is focused on the vidicon target through the shutter, which is placed slightly in front of the focal plane. The vidicon target is made up of a layer of photoconductive material, initially charged by scanning with an electron beam. The image formed on the photoconductive surface causes variations in resistance across the surface which are a function of the image brightness. These variations allow a redistribution of the charge which remains after exposure. In the *Ranger* cameras, the charge pattern formed by the image on the photoconductor remains much longer than in commercial systems, so that the pictures may be taken more slowly. By slowing down the picture-taking rate, it is possible to use a narrow electrical bandwidth, which simplifies the communications problem in transmission of the signal to Earth. After the image has been formed on the photoconductor by operation of the shutter, an electron beam scans the surface and recharges the photoconductor. The variation in charge current is the video signal, which is then amplified several thousand times and sent to the transmitter, where the amplitude variations are converted to frequency variations. The frequency-modulated signal is amplified, and the signals from the two channels are combined and transmitted to Earth through the spacecraft high-gain antenna.

1. F Channel

The F channel has two cameras—the A camera with a 25° field and the B camera with an 8.4° field. Both have 5-msec exposure times; however, the A camera has a 25-mm f/1.0 lens, while the B camera f/20 lens is 76 mm. The combined useful operating range of the two cameras is from about 10 to 1500 ft-L* scene brightness. This large dynamic range allows for the possibility of the spacecraft impacting in a region with poor lighting conditions without appreciable reduction in the quality of the photographs. The electron beam scans an area approximately 11 mm square in 2.5 sec with 1150 lines.

The two cameras operate in sequence, so that only one camera is being scanned at a particular time. This allows the signals from the two cameras to be transmitted over a single transmitter. Since each camera requires 2.5 sec to be scanned and then must wait 2.5 sec while the other camera is scanned, there are intervals of about 5 sec between consecutive pictures on a particular camera. During the waiting period, the cameras erase the residual image from the preceding picture and the shutter exposes the vidicon for the next cycle of operation.

2. P Channel

The P channel contains four cameras, designated P_1 through P_4. The same combination of lens types as in the F channel is used in the P cameras. P_1 and P_2 use 76-mm f/2.0 lenses, and P_3 and P_4 use 25-mm f/1.0 lenses, so that the P cameras have the same dynamic range capability as the F cameras. The primary difference between the two sets of cameras is in the scan rates and the portion of the photoconductive target used. The P cameras scan only a 2.8-mm-square segment of the target with 300 scan lines. The time required to scan the area is 0.2 sec. Again, as with the F cameras, only one camera is being scanned at a time, so that all four are coupled into a single transmitter. The time between consecutive pictures on a particular camera is 0.84 sec. Because of the smaller target area of the P cameras, the field of view is correspondingly smaller than that of the F cameras. P_1 and P_2 have approximately 2.1° fields, while the P_3 and P_4 fields are approximately 6.3°. In addition to the differences described above, the P-camera exposure times are shorter than the F exposures. The P shutters are set for a 2-msec exposure to reduce image motion as the spacecraft approaches the lunar surface. The last complete F-camera picture is taken between 2.5 and 5 sec before impact, while the last complete P-camera picture is taken between 0.2 and 0.4 sec because of the faster cycling rate on the P cameras. Image motion is therefore more severe in the last P camera pictures, and shorter exposure times are required. The sequence for one cycle of operation of the P cameras is P_1–P_3–P_2–P_4, so that photographs are taken alternately by a 76-mm lens and a 25-mm lens.

B. Receiving and Recording Equipment

The television signals from the spacecraft are received with 85-ft-diameter antennas at two sites, located about 10 mi apart at Goldstone, California. The signals are amplified and mixed by a local oscillator to reduce the signal center frequency to 30 Mc and then sent to the television receiver. Another mixing operation reduces the

*1 ft-L = 1.0764×10^{-3} lamberts.

frequency to 4.5 and 5.5 Mc, respectively, for the two channels. The signal frequency variations are then converted back to amplitude variations in two demodulators (one for each camera channel), whose outputs are the same as the video signals originally generated in the cameras. The video signals are used to control the intensity of an electron beam in a cathode-ray tube, which is scanned in unison with the electron beam in the cameras. The cathode-ray tube reconstructs the original image, which is then photographed on 35-mm film. These recording devices are similar to the commercial kinescopes used for recording television programs on film. Again, there is one recording device for each camera channel, so that two pictures are being recorded at any instant in time, one F camera and one P camera. All the functions discussed above are duplicated at both receiving sites, with one exception. One site utilizes a single film recorder to record the four P cameras, while the other site maintains two film recorders and records both camera channels.

In addition to the film recorders, another means of recording the data is used. The 4.5- and 5.5-Mc signals that go to the demodulators are also sent to another mixer, which reduces the center frequency still further to 500 kc. These signals are recorded on magnetic tape at both sites. Two such recorders are used at each receiving station. In order to obtain film records from the magnetic tapes, they are played through a demodulator, and the video signal is applied to the film recorder as discussed above.

C. Camera Calibration

The calibration of the cameras involves three principal aspects of camera performance: light-transfer characteristic (photometric calibration), sine-wave response (modulation transfer function), and system noise. In addition, data on geometric distortion are obtained.

Subsequent to the *Ranger VII* mission, the f/2-camera video amplifiers were adjusted to increase the video amplification. This adjustment reduced the peak illumination which could be accepted; however, since both *Ranger VIII* and *IX* were targeted within 15° of the terminator, the expected scene brightness was well within the dynamic range of the cameras. Figure 4 shows a typical light-transfer characteristic with the adjusted amplification. The adjustment provided a slight improvement in signal-to-noise ratio in the received pictures.

1. Light-Transfer Characteristic

In order to obtain some absolute photometric information about the lunar surface, camera sensitivity is measured as a function of scene brightness. Using a set of collimators to simulate the scene, the cameras are exposed to various brightness levels before launch, and the camera signal output is recorded on magnetic tape. The magnetic tape is then played back through the recording equipment at Goldstone, and the calibration data are recorded on the same film as the lunar photographs in order to eliminate errors due to differences in film strips processed at different times. The variation in development of a single strip from one end to the other is negligible. The net result, then, is the functional relationship between film density and collimator brightness. In order to account for the differences between the spectral emission characteristics of the collimators and the reflected solar radiation from the lunar scene, a series of spectral measurements is made on all the instrumentation. A correction factor is then calculated to correct the collimator brightness to lunar scene brightness. Reference 5 describes this procedure. Since the photometric calibration is on the same film as the photographic data, it can be carried through subsequent copying operations. A typical light-transfer characteristic of scene brightness vs. negative film density for a 76-mm and a 25-mm camera is shown in Fig. 4. The accuracy of the photo-

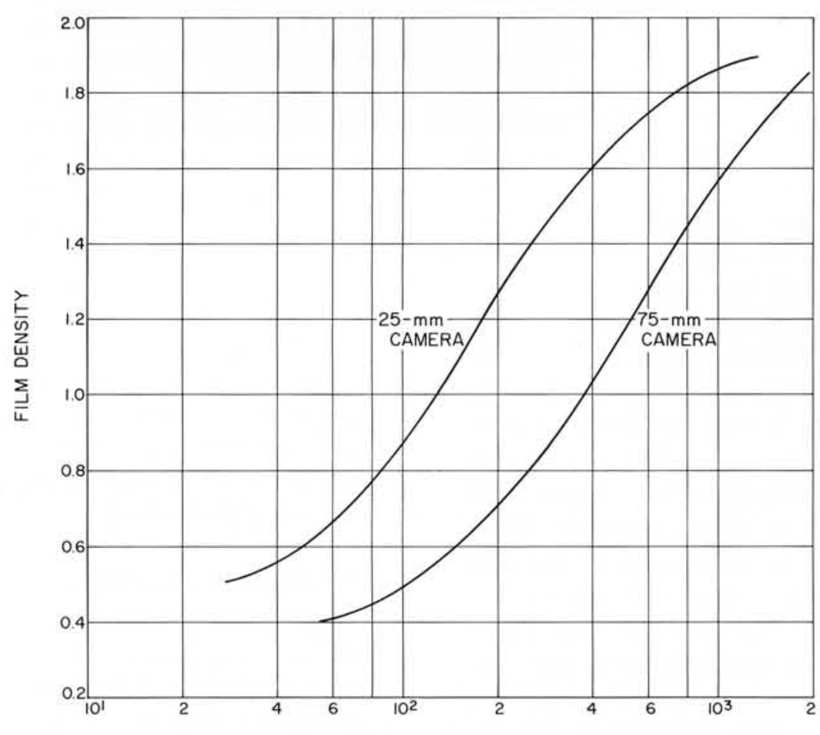

Fig. 4. Typical light-transfer characteristics

metric calibration is limited primarily by vidicon nonuniformities and variations in exposure times, and is expected to be about ±20%.

2. Sine-Wave Response

In order to obtain the approximate mathematical description of the system required for the figure of merit, it is necessary to determine the sine-wave response of the system. There are a number of ways of obtaining such data. The most direct method is the use of slides with sinusoidal variations in transmission which are then placed in the calibration collimators to illuminate the cameras. A film recording is made, and then the film is scanned with a microphotometer to determine the sine-wave response. A typical response curve is shown in Fig. 5.

3. System Noise and Geometric Distortion

Noise is one of the critical parameters of a photographic system which is required to characterize the system. For a television system, it is convenient to combine film granularity with electrical noise generated in the camera and the communication system to obtain an over-all measure of system noise. The over-all noise is measured by scanning a film recording with a microphotometer. The resulting record is then analyzed to calculate the root-mean-square variations in transmission.

Geometric distortion is determined by inserting a slide in the collimators which has been ruled horizontally and vertically. Photographs of the slide are then used to correct the distortion.

D. Film Processing

The film used in the *Ranger* missions was Eastman Kodak television recording film, type 5374. The negatives were developed by a commercial film processor* to a gamma of 1.4. The photographs in this volume were made using the following procedure:

1. The magnetic tape recorded during the mission was replayed and recorded on film.
2. 8 × 10-in. positives of Du Pont Commercial S film were prepared by enlarging the 35-mm negatives, using some manual dodging.
3. The 8 × 10-in. positives were contact-printed, and the same film was used to prepare negatives.
4. The photographs were contact-printed from the negatives, with some additional dodging done in the contact printer.

*Consolidated Film Industries, Hollywood, California.

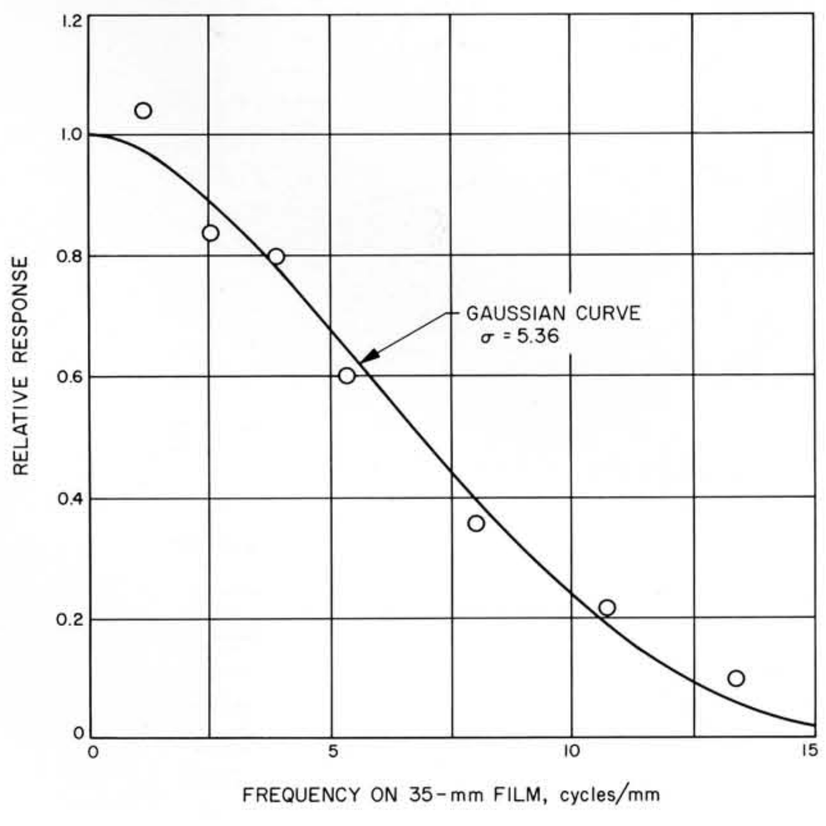

Fig. 5. Typical sine-wave response

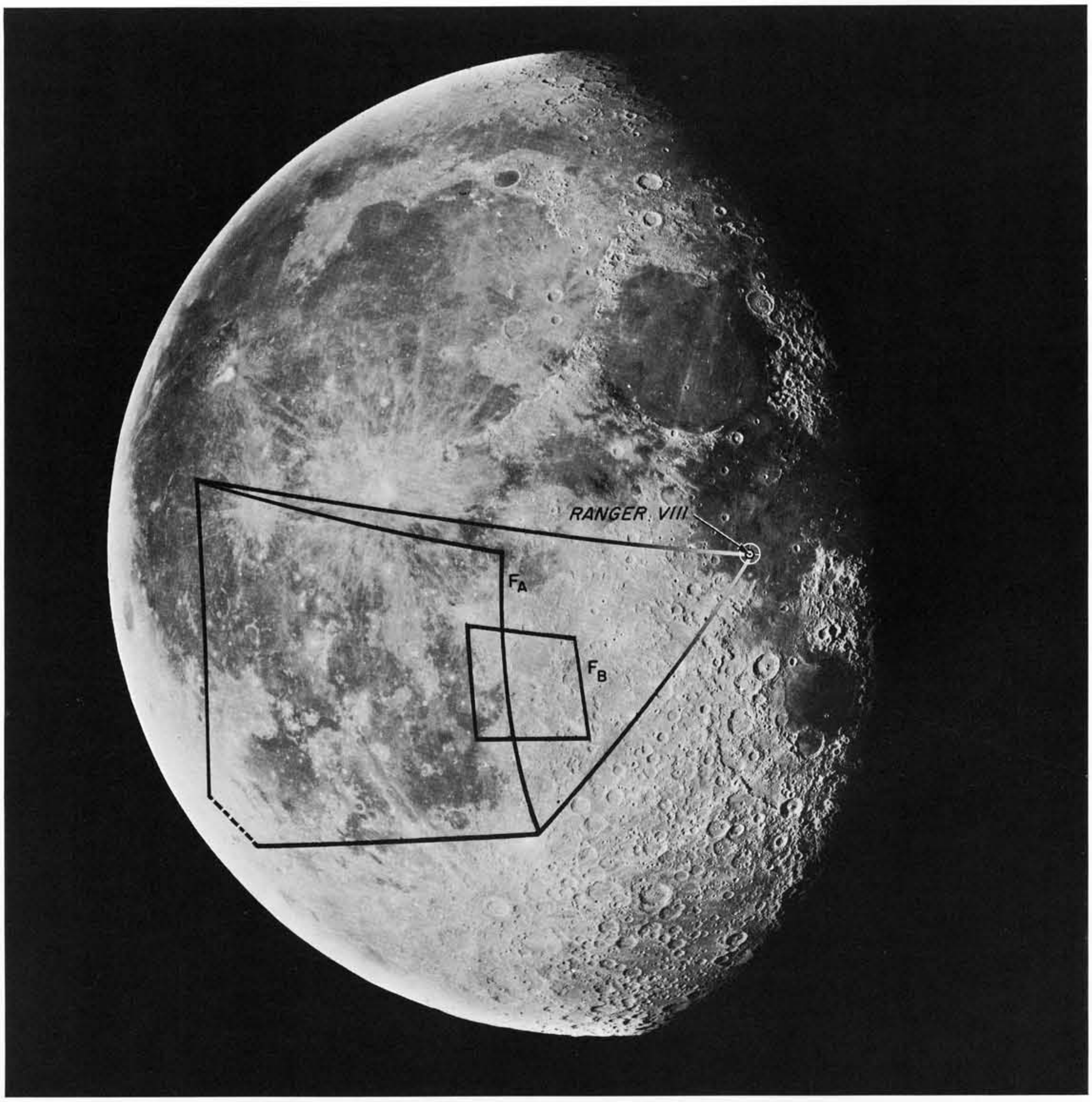

Fig. 6. *Ranger VIII* area coverage

V. CAMERA TABLES OF VALUES

The lunar area photographed by the *Ranger VIII* cameras is shown in Fig. 6*, and the areas covered by the initial pictures from the full-scan A and B cameras are outlined.

Repetition of some permanent camera surface characteristics will be noted in each frame. These irregularities should be ignored in any photograph interpretation studies.

The parameters listed in the preliminary tables of values (Table 2) are defined below:

Spacecraft

Altitude: The distance from the spacecraft to the surface directly below.

Latitude, longitude: The selenocentric position of the point of intersection with the surface of a line connecting the spacecraft and the center of the Moon. This defines the surface point directly below the spacecraft.

*Lick Observatory photograph.

Photograph

Central reticle: The principal cross mark on the camera face (Fig. 7).

Latitude, longitude: The surface point in selenocentric coordinates covered by the central reticle.

Slant range: The distance from the spacecraft to the surface point covered by the central reticle (Fig. 8).

Incidence, phase, emission angles: The emission angle is the angle between the local surface normal and the camera axis. The incidence angle is the angle between the local surface normal and the direction of illumination. The phase angle is measured between the illumination direction and the camera axis. These three angles form the photometric geometry. They can be oriented by noting that the direction of illumination of the observed point is parallel to the line passing through the subsolar point and the Moon center (neglecting parallax) and that the emission angle is measured in the plane formed by the spacecraft surface point

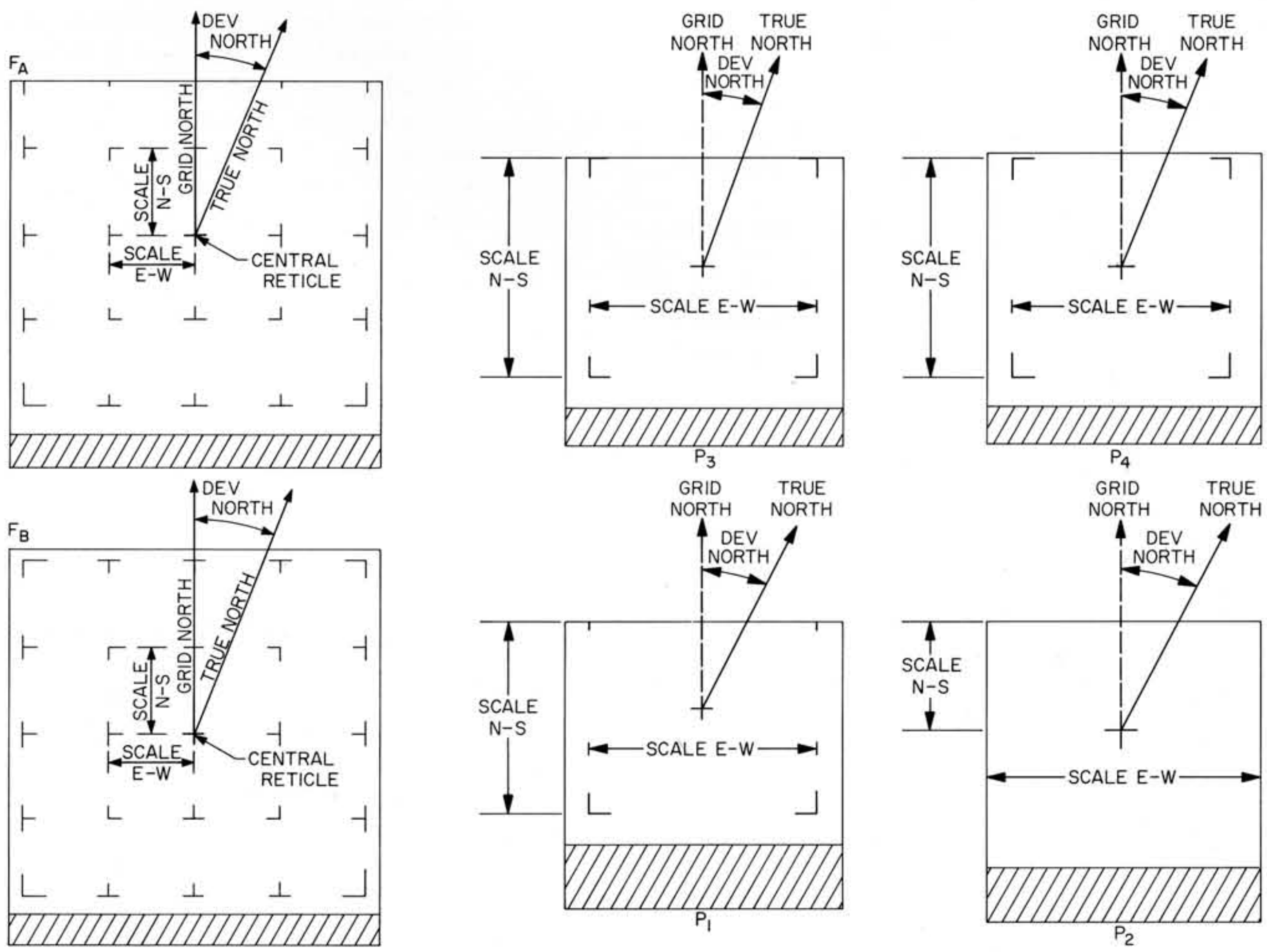

Fig. 7. Definition of central reticle, deviation north, and scale

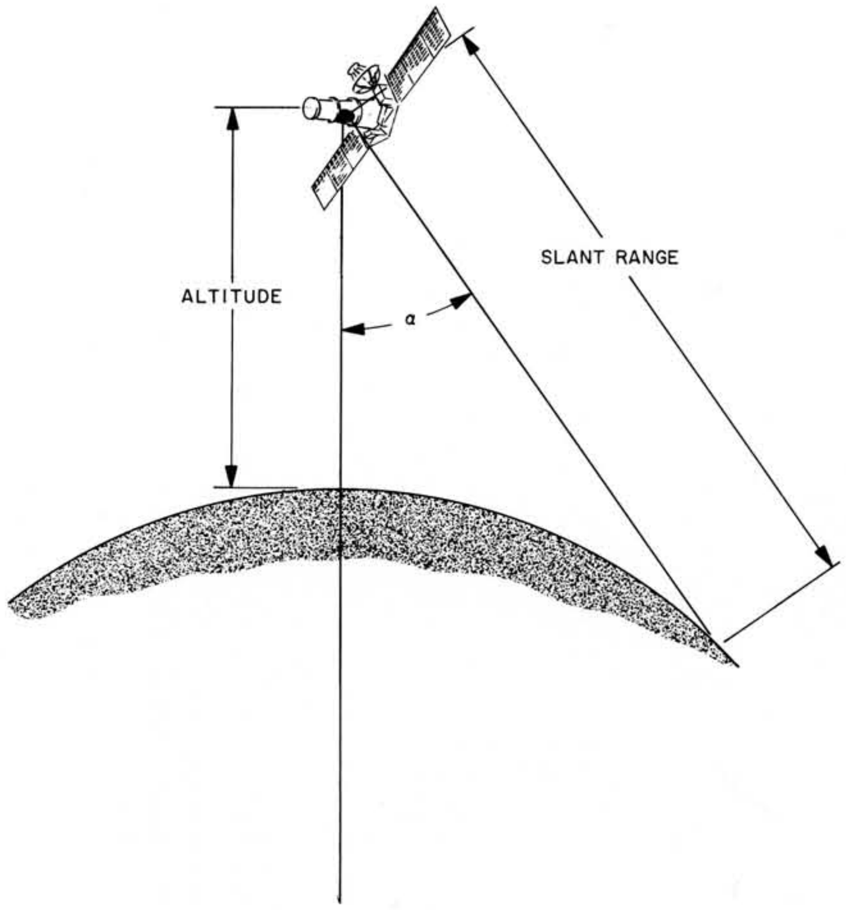

Fig. 8. Altitude and range definition

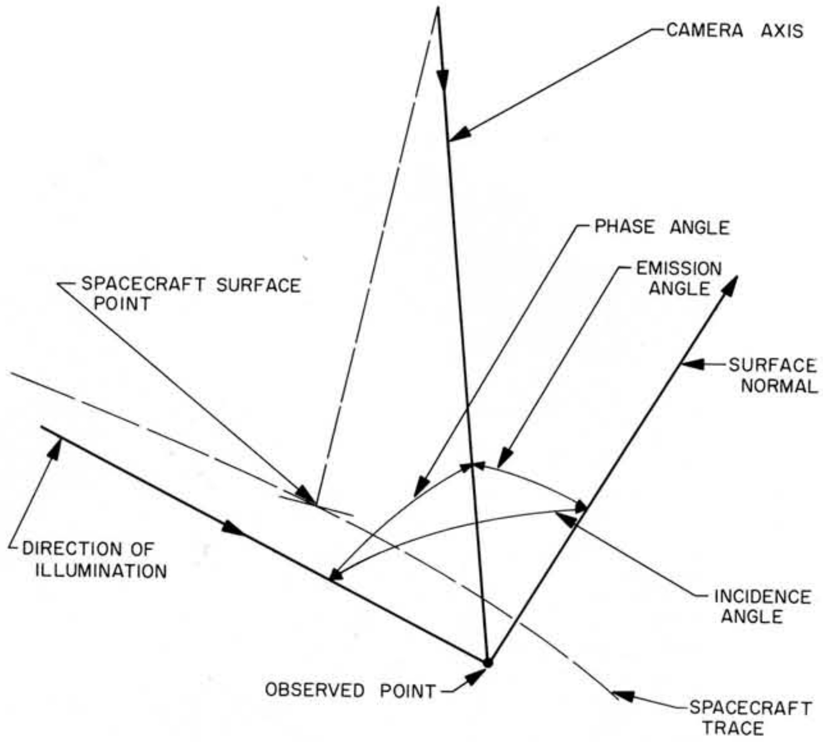

Fig. 9. *Ranger VIII* photometric geometry

and the local normal (Fig. 9). For *Ranger VIII,* the subsolar point was at −1.48° latitude and −50.47° longitude.

Scale (E-W, N-S): The distances between the surface points covered by the reticles are indicated in Fig. 7.

Deviation north: Grid north is defined by a straight line drawn from the central reticle to the middle reticle in the north margin of the A- and B-camera photographs. For the P-camera pictures, grid north is defined by a straight line, parallel to the reticle pattern or the edge of the picture, drawn from the central reticle toward the north margin of the photograph. The deviation is the clockwise rotation from grid north to the direction of true north at the central reticle. Convergence of the meridians is appreciable in all but the P_1- and P_2-camera photographs, including the larger-scale pictures, and directions at the central reticles cannot be transferred to the left and right margins without introducing errors (Fig. 7).

Table 2. *Ranger VIII* preliminary tables of values
a. Camera A

Photo number	GMT of frame exposure Feb. 20, 1965	Spacecraft			Photograph (central reticle)						Scale, km		Deviation north, deg
		Altitude, km	Latitude, deg	Longitude, deg	Latitude, deg	Longitude, deg	Slant range, km	Incidence angle, deg	Phase angle, deg	Emission angle, deg	E-W	N-S	
1	09:34:32.272	2510.27	−7.24	−10.76	−10.65	−22.42	2573.72	29.1	47.3	20.1	283.32	243.87	−6.2
2	09:41:01.391	1820.93	−5.95	−5.88	−7.25	−8.24	1826.22	41.8	47.3	6.2	176.96	172.47	−3.3
3	09:45:48.109	1301.11	−4.58	−0.85	−4.43	0.85	1302.91	51.2	47.3	4.0	121.81	123.40	−2.2
4	09:48:57.549	952.72	−3.34	3.54	−2.51	7.23	963.35	57.6	47.3	10.6	89.67	91.70	−2.0
5	09:50:45.068	753.79	−2.48	6.57	−1.39	10.86	770.69	61.3	47.3	14.4	72.01	73.67	−2.1
6	09:51:15.788	696.88	−2.21	7.53	−1.07	11.90	715.42	62.3	47.3	15.5	66.97	68.48	−2.2
7	09:51:46.508	639.96	−1.92	8.53	−0.75	12.94	660.03	63.3	47.3	16.6	61.92	63.27	−2.3
8	09:52:12.108	592.54	−1.67	9.41	−0.49	13.81	613.72	64.2	47.3	17.5	57.71	58.91	−2.3
9	09:52:37.708	545.14	−1.40	10.32	−0.22	14.68	567.25	65.1	47.3	18.5	53.47	54.53	−2.4
10	09:53:03.308	497.78	−1.13	11.26	0.03	15.54	520.53	66.0	47.3	19.4	49.20	50.11	−2.5
11	09:53:23.788	459.93	−0.90	12.05	0.24	16.23	483.02	66.7	47.3	20.1	45.76	46.55	−2.6
12	09:53:28.908	450.47	−0.84	12.25	0.29	16.41	473.61	66.9	47.3	20.3	44.90	45.66	−2.6
13	09:53:34.028	441.01	−0.79	12.46	0.34	16.59	464.20	67.0	47.3	20.4	44.04	44.77	−2.6
14	09:53:39.148	431.56	−0.73	12.66	0.39	16.75	454.78	67.2	47.3	20.6	43.17	43.87	−2.7
15	09:53:44.268	422.12	−0.67	12.87	0.44	16.93	445.36	67.4	47.3	20.8	42.31	42.98	−2.7
16	09:53:49.388	412.67	−0.61	13.08	0.50	17.10	435.92	67.6	47.3	21.0	41.44	42.08	−2.7
17	09:53:54.508	403.23	−0.54	13.29	0.55	17.27	426.46	67.7	47.3	21.2	40.57	41.18	−2.7
18	09:53:59.628	393.79	−0.48	13.50	0.60	17.44	416.99	67.9	47.3	21.4	39.69	40.28	−2.7
19	09:54:04.747	384.36	−0.42	13.71	0.65	17.62	407.51	68.1	47.3	21.5	38.82	39.38	−2.8
20	09:54:09.867	374.93	−0.36	13.93	0.70	17.79	398.02	68.3	47.3	21.7	37.94	38.47	−2.8
21	09:54:14.987	365.50	−0.30	14.15	0.75	17.96	388.52	68.4	47.3	21.9	37.06	37.57	−2.8
22	09:54:20.107	356.08	−0.23	14.37	0.80	18.13	379.01	68.6	47.3	22.1	36.18	36.66	−2.8
23	09:54:25.227	346.66	−0.17	14.59	0.86	18.31	369.48	68.8	47.3	22.3	35.30	35.75	−2.9
24	09:54:30.347	337.25	−0.10	14.81	0.91	18.48	359.94	69.0	47.3	22.4	34.41	34.84	−2.9
25	09:54:35.467	327.84	−0.04	15.04	0.96	18.65	350.39	69.1	47.3	22.6	33.52	33.93	−2.9
26	09:54:40.587	318.44	0.03	15.27	1.01	18.82	340.82	69.3	47.3	22.8	32.63	33.01	−2.9
27	09:54:45.707	309.05	0.10	15.50	1.06	18.99	331.23	69.5	47.3	23.0	31.74	32.09	−3.0
28	09:54:50.827	299.65	0.16	15.73	1.11	19.17	321.63	69.7	47.3	23.2	30.84	31.17	−3.0
29	09:54:55.947	290.27	0.23	15.97	1.16	19.34	312.02	69.8	47.3	23.3	29.95	30.25	−3.0
30	09:55:01.067	280.89	0.30	16.20	1.22	19.51	302.39	70.0	47.3	23.5	29.05	29.33	−3.0
31	09:55:06.187	271.52	0.37	16.44	1.27	19.68	292.75	70.2	47.3	23.7	28.14	28.41	−3.1
32	09:55:11.307	262.15	0.44	16.68	1.32	19.85	283.09	70.3	47.3	23.9	27.24	27.48	−3.1
33	09:55:16.427	252.79	0.51	16.93	1.37	20.02	273.42	70.5	47.3	24.1	26.33	26.55	−3.1
34	09:55:21.547	243.44	0.58	17.17	1.42	20.19	263.73	70.7	47.3	24.2	25.42	25.62	−3.2
35	09:55:26.667	234.09	0.65	17.42	1.47	20.36	254.02	70.9	47.3	24.4	24.50	24.69	−3.2
36	09:55:31.787	224.75	0.72	17.67	1.52	20.53	244.29	71.0	47.3	24.6	23.58	23.75	−3.2
37	09:55:36.907	215.42	0.80	17.92	1.57	20.71	234.54	71.2	47.3	24.8	22.66	22.81	−3.3
38	09:55:42.027	206.10	0.87	18.18	1.62	20.88	224.78	71.4	47.3	25.0	21.74	21.87	−3.3
39	09:55:47.147	196.79	0.95	18.44	1.67	21.05	214.99	71.6	47.3	25.1	20.81	20.93	−3.3
40	09:55:52.267	187.48	1.02	18.70	1.72	21.22	205.19	71.7	47.3	25.3	19.88	19.98	−3.3
41	09:55:57.387	178.19	1.10	18.96	1.77	21.39	195.36	71.9	47.3	25.5	18.95	19.03	−3.4
42	09:56:02.507	168.90	1.17	19.22	1.82	21.55	185.51	72.1	47.3	25.7	18.01	18.08	−3.4
43	09:56:07.627	159.62	1.25	19.49	1.87	21.72	175.65	72.2	47.3	25.8	17.07	17.12	−3.4
44	09:56:12.747	150.35	1.33	19.76	1.92	21.89	165.76	72.4	47.3	26.0	16.12	16.17	−3.4
45	09:56:17.867	141.10	1.41	20.04	1.97	22.06	155.84	72.6	47.3	26.2	15.17	15.21	−3.5
46	09:56:22.987	131.85	1.49	20.31	2.02	22.23	145.91	72.8	47.3	26.4	14.22	14.24	−3.5
47	09:56:28.107	122.61	1.57	20.59	2.07	22.40	135.96	72.9	47.3	26.5	13.26	13.28	−3.5
48	09:56:33.227	113.39	1.65	20.87	2.12	22.57	125.98	73.1	47.3	26.7	12.30	12.31	−3.6
49	09:56:38.347	104.17	1.73	21.16	2.17	22.73	115.97	73.3	47.3	26.9	11.34	11.33	−3.6
50	09:56:43.467	94.97	1.81	21.45	2.22	22.90	105.95	73.4	47.3	27.1	10.37	10.36	−3.6
51	09:56:48.587	85.78	1.90	21.74	2.27	23.07	95.90	73.6	47.3	27.3	9.39	9.38	−3.6
52	09:56:53.707	76.60	1.98	22.03	2.31	23.23	85.82	73.8	47.3	27.4	8.42	8.40	−3.7
53	09:56:58.827	67.44	2.07	22.33	2.36	23.40	75.72	73.9	47.3	27.6	7.43	7.41	−3.7
54	09:57:03.947	58.29	2.15	22.63	2.41	23.67	65.59	74.1	47.3	27.8	6.44	6.42	−3.7
55	09:57:09.067	49.15	2.24	22.93	2.46	23.73	55.43	74.3	47.3	27.9	5.45	5.43	−3.8
56	09:57:14.187	40.03	2.32	23.23	2.51	23.90	45.24	74.4	47.3	28.1	4.46	4.43	−3.8
57	09:57:19.307	30.92	2.41	23.54	2.56	24.06	35.03	74.6	47.3	28.3	3.45	3.43	−3.8
58	09:57:24.427	21.83	2.50	23.86	2.61	24.23	24.79	74.8	47.3	28.5	2.45	2.43	−3.8
59	09:57:29.547	12.74	2.59	24.17	2.65	24.39	14.51	74.9	47.3	28.6	1.43	1.42	−3.9
60	09:57:34.667	3.69	2.68	24.49	2.70	24.55	4.21	75.1	47.3	28.8	0.42	0.41	−3.9
IMPACT	09:57:36.756												

Table 2. (Cont'd)
b. Camera B

Photo number	GMT of frame exposure Feb. 20, 1965	Spacecraft			Photograph (central reticle)						Scale, km		Deviation north, deg
		Altitude, km	Latitude, deg	Longitude, deg	Latitude, deg	Longitude, deg	Slant range, km	Incidence angle, deg	Phase angle, deg	Emission angle, deg	E-W	N-S	
1	09:34:34.832	2505.79	−7.23	−10.74	−11.78	−2.31	2545.50	48.7	34.0	15.9	86.54	84.81	−0.8
2	09:36:22.352	2317.13	−6.92	−9.55	−10.75	−0.06	2363.93	50.7	33.9	17.5	81.18	78.68	−0.6
3	09:38:09.871	2127.07	−6.58	−8.25	−9.66	2.10	2181.11	52.7	34.0	19.2	75.70	72.53	−0.5
4	09:39:42.031	1963.03	−6.26	−7.02	−8.70	4.05	2024.83	54.6	34.0	20.9	71.08	67.31	−0.5
5	09:41:09.070	1807.14	−5.92	−5.76	−7.78	5.84	1876.08	56.3	34.0	22.4	66.60	62.36	−0.6
6	09:42:25.870	1668.81	−5.59	−4.56	−6.95	7.42	1744.17	57.8	34.0	23.9	62.59	57.99	−0.8
7	09:43:42.670	1529.75	−5.24	−3.25	−6.13	9.03	1611.88	59.4	34.0	25.5	58.55	53.62	−0.9
8	09:44:49.230	1408.66	−4.90	−2.02	−5.41	10.39	1495.88	60.7	34.0	26.8	54.91	49.79	−1.1
9	09:45:19.950	1352.60	−4.73	−1.42	−5.07	11.03	1442.16	61.4	34.0	27.4	53.22	48.03	−1.2
10	09:45:50.669	1296.43	−4.56	−0.80	−4.72	11.67	1388.36	62.0	34.0	28.0	51.53	46.26	−1.3
11	09:46:21.389	1240.16	−4.38	−0.16	−4.39	12.31	1334.25	62.7	34.0	28.7	49.80	44.48	−1.4
12	09:46:46.989	1193.20	−4.23	0.40	−4.12	12.84	1288.77	63.2	34.0	29.2	48.33	42.98	−1.5
13	09:47:07.469	1155.58	−4.10	0.86	−3.90	13.25	1252.23	63.6	34.0	29.6	47.13	41.78	−1.6
14	09:47:27.949	1117.91	−3.97	1.33	−3.67	13.67	1215.63	64.0	34.0	30.1	45.93	40.58	−1.7
15	09:47:48.429	1080.22	−3.83	1.81	−3.45	14.09	1178.94	64.4	34.0	30.5	44.73	39.37	−1.8
16	09:48:08.909	1042.48	−3.69	2.30	−3.22	14.52	1142.12	64.9	34.0	30.9	43.51	38.16	−1.9
17	09:48:29.389	1004.71	−3.55	2.81	−3.00	14.94	1105.14	65.3	34.0	31.4	42.28	36.95	−2.0
18	09:48:49.869	966.90	−3.40	3.34	−2.77	15.36	1067.99	65.7	34.0	31.8	41.03	35.73	−2.1
19	09:49:05.229	938.53	−3.29	3.74	−2.60	15.67	1039.95	66.0	34.0	32.1	40.08	34.81	−2.1
20	09:49:20.589	910.14	−3.17	4.15	−2.43	15.98	1011.75	66.3	34.0	32.4	39.11	33.88	−2.2
21	09:49:35.949	881.74	−3.05	4.57	−2.26	16.28	983.45	66.6	34.0	32.8	38.14	32.95	−2.3
22	09:49:51.308	853.33	−2.93	5.00	−2.09	16.59	955.12	67.0	34.0	33.1	37.16	32.01	−2.4
23	09:50:06.668	824.90	−2.81	5.43	−1.92	16.90	926.55	67.3	34.0	33.4	36.16	31.07	−2.5
24	09:50:22.028	796.46	−2.68	5.88	−1.76	17.21	898.06	67.6	34.0	33.7	35.18	30.14	−2.6
25	09:50:37.388	768.02	−2.55	6.34	−1.59	17.52	869.32	67.9	34.0	34.1	34.16	29.19	−2.7
26	09:50:47.628	749.05	−2.46	6.65	−1.47	17.72	850.10	68.1	34.0	34.3	33.49	28.55	−2.7
27	09:50:57.868	730.08	−2.37	6.96	−1.36	17.92	830.76	68.3	34.0	34.5	32.80	27.92	−2.8
28	09:51:08.108	711.10	−2.28	7.28	−1.25	18.11	811.33	68.5	34.0	34.7	32.10	27.27	−2.8
29	09:51:18.348	692.14	−2.18	7.61	−1.14	18.32	791.91	68.7	34.0	34.9	31.40	26.63	−2.9
30	09:51:28.588	673.16	−2.09	7.94	−1.03	18.52	772.41	68.9	34.0	35.1	30.70	25.99	−3.0
31	09:51:38.828	654.19	−1.99	8.28	−0.91	18.72	752.84	69.1	34.0	35.3	29.99	25.34	−3.0
32	09:51:49.068	635.22	−1.89	8.62	−0.80	18.92	733.20	69.3	34.0	35.5	29.27	24.69	−3.1
33	09:51:59.308	616.25	−1.79	8.96	−0.69	19.12	713.47	69.5	34.0	35.8	28.55	24.04	−3.2
34	09:52:09.548	597.28	−1.69	9.32	−0.58	19.32	693.67	69.7	34.0	36.0	27.83	23.38	−3.2
35	09:52:19.788	578.32	−1.59	9.68	−0.47	19.51	673.82	69.9	34.0	36.2	27.09	22.73	−3.3
36	09:52:30.028	559.36	−1.48	10.04	−0.36	19.71	653.83	70.1	34.0	36.4	26.35	22.06	−3.4
37	09:52:40.268	540.40	−1.38	10.41	−0.25	19.90	633.74	70.3	34.0	36.6	25.60	21.39	−3.4
38	09:52:50.508	521.45	−1.27	10.79	−0.15	20.09	613.54	70.5	34.0	36.8	24.84	20.72	−3.5
39	09:53:00.748	502.51	−1.16	11.17	−0.04	20.28	593.27	70.7	34.0	37.0	24.07	20.05	−3.6
40	09:53:10.988	483.58	−1.05	11.56	0.07	20.47	572.92	70.9	34.0	37.2	23.30	19.37	−3.6
41	09:53:21.228	464.65	−0.93	11.95	0.17	20.66	552.47	71.1	34.0	37.4	22.52	18.69	−3.7
42	09:53:26.348	455.20	−0.87	12.15	0.23	20.75	542.21	71.2	34.0	37.5	22.13	18.35	−3.7
43	09:53:31.468	445.74	−0.81	12.36	0.28	20.84	531.92	71.3	34.0	37.6	21.74	18.00	−3.8
44	09:53:36.588	436.29	−0.76	12.56	0.33	20.93	521.60	71.4	34.0	37.7	21.34	17.66	−3.8
45	09:53:41.708	426.84	−0.70	12.77	0.38	21.03	511.27	71.5	34.0	37.8	20.94	17.31	−3.8
46	09:53:46.828	417.39	−0.64	12.97	0.44	21.12	500.92	71.6	34.0	37.9	20.54	16.97	−3.9
47	09:53:51.948	407.95	−0.58	13.18	0.49	21.21	490.54	71.7	34.0	38.0	20.14	16.62	−3.9
48	09:53:57.067	398.51	−0.51	13.39	0.54	21.30	480.11	71.8	34.0	38.1	19.73	16.27	−4.0
49	09:54:02.187	389.07	−0.45	13.61	0.60	21.39	469.64	71.9	34.0	38.2	19.33	15.92	−4.0
50	09:54:07.307	379.64	−0.39	13.82	0.65	21.48	459.16	71.9	34.0	38.3	18.92	15.57	−4.0
51	09:54:12.427	370.21	−0.33	14.04	0.70	21.57	448.66	72.0	34.0	38.4	18.50	15.22	−4.1
52	09:54:17.547	360.79	−0.26	14.26	0.75	21.66	438.12	72.1	34.0	38.5	18.09	14.86	−4.1
53	09:54:22.667	351.37	−0.20	14.48	0.81	21.75	427.56	72.2	34.0	38.6	17.68	14.51	−4.1
54	09:54:27.787	341.96	−0.14	14.70	0.86	21.84	416.97	72.3	34.0	38.7	17.26	14.15	−4.2
55	09:54:32.907	332.55	−0.07	14.93	0.91	21.93	406.34	72.4	34.0	38.8	16.84	13.80	−4.2
56	09:54:38.027	323.14	0.00	15.15	0.96	22.01	395.68	72.5	34.0	38.9	16.41	13.44	−4.2
57	09:54:43.147	313.74	0.06	15.38	1.02	22.10	384.99	72.6	34.0	38.9	15.99	13.08	−4.3
58	09:54:48.267	304.35	0.13	15.61	1.07	22.18	374.26	72.7	34.0	39.0	15.56	12.72	−4.3
59	09:54:53.387	294.96	0.20	15.85	1.12	22.27	363.50	72.8	34.0	39.1	15.13	12.36	−4.4
60	09:54:58.507	285.58	0.27	16.08	1.17	22.36	352.72	72.8	34.0	39.2	14.70	11.99	−4.4
61	09:55:03.627	276.20	0.33	16.32	1.23	22.44	341.90	72.9	34.0	39.3	14.26	11.63	−4.4
62	09:55:08.747	266.83	0.40	16.56	1.28	22.52	331.05	73.0	34.0	39.4	13.82	11.26	−4.5
63	09:55:13.867	257.47	0.47	16.80	1.33	22.61	320.17	73.1	34.0	39.5	13.38	10.90	−4.5
64	09:55:18.987	248.11	0.54	17.05	1.38	22.70	309.24	73.2	34.0	39.6	12.94	10.53	−4.6

Table 2b. (Cont'd)

Photo number	GMT of frame exposure Feb. 20, 1965	Spacecraft			Photograph (central reticle)						Scale, km		Deviation north, deg
		Altitude, km	Latitude, deg	Longitude, deg	Latitude, deg	Longitude, deg	Slant range, km	Incidence angle, deg	Phase angle, deg	Emission angle, deg	E-W	N-S	
65	09:55:24.107	238.76	0.62	17.29	1.43	22.77	298.29	73.3	34.0	39.7	12.50	10.16	−4.6
66	09:55:29.227	229.42	0.69	17.54	1.49	22.85	287.29	73.4	34.0	39.8	12.05	9.79	−4.6
67	09:55:34.347	220.09	0.76	17.80	1.54	22.93	276.26	73.4	34.0	39.9	11.60	9.42	−4.7
68	09:55:39.467	210.76	0.83	18.05	1.59	23.01	265.19	73.5	34.0	39.9	11.15	9.04	−4.7
69	09:55:44.587	201.44	0.91	18.31	1.64	23.09	254.08	73.6	34.0	40.0	10.69	8.66	−4.8
70	09:55:49.707	192.13	0.98	18.57	1.69	23.17	242.94	73.7	34.0	40.1	10.23	8.29	−4.8
71	09:55:54.827	182.83	1.06	18.83	1.74	23.25	231.75	73.8	34.0	40.2	9.77	7.91	−4.8
72	09:55:59.947	173.54	1.13	19.09	1.79	23.33	220.53	73.8	34.0	40.3	9.31	7.53	−4.9
73	09:56:05.067	164.26	1.21	19.36	1.84	23.40	209.26	73.9	34.0	40.4	8.84	7.15	−4.9
74	09:56:10.187	154.99	1.29	19.63	1.89	23.48	197.95	74.0	34.0	40.5	8.37	6.76	−5.0
75	09:56:15.307	145.72	1.37	19.90	1.94	23.55	168.60	74.1	34.0	40.5	7.90	6.38	−5.0
76	09:56:20.427	136.47	1.45	20.17	1.99	23.63	175.21	74.2	34.0	40.6	7.43	5.99	−5.0
77	09:56:25.547	127.23	1.53	20.45	2.04	23.70	163.78	74.2	34.0	40.7	6.95	5.60	−5.1
78	09:56:30.667	118.00	1.61	20.73	2.09	23.77	152.31	74.3	34.0	40.8	6.47	5.21	−5.1
79	09:56:35.787	108.78	1.69	21.02	2.14	23.84	140.79	74.4	34.0	40.9	5.99	4.82	−5.1
80	09:56:40.907	99.57	1.77	21.30	2.19	23.91	129.22	74.4	34.0	40.9	5.50	4.42	−5.2
81	09:56:46.027	90.37	1.85	21.59	2.24	23.98	117.62	74.5	34.0	41.0	5.01	4.03	−5.2
82	09:56:51.147	81.19	1.94	21.88	2.29	24.05	105.96	74.6	34.0	41.1	4.52	3.63	−5.2
83	09:56:56.267	72.02	2.02	22.18	2.34	24.12	94.26	74.7	34.0	41.2	4.02	3.23	−5.3
84	09:57:01.387	62.86	2.11	22.48	2.39	24.19	82.51	74.7	34.0	41.2	3.53	2.83	−5.3
85	09:57:06.507	53.72	2.19	22.78	2.44	24.25	70.72	74.8	34.0	41.3	3.02	2.42	−5.3
86	09:57:11.627	44.59	2.28	23.08	2.48	24.32	58.87	74.9	34.0	41.4	2.52	2.02	−5.4
87	09:57:16.747	35.47	2.37	23.39	2.53	24.38	46.97	74.9	34.0	41.5	2.01	1.61	−5.4
88	09:57:21.867	26.37	2.46	23.70	2.58	24.44	35.03	75.0	34.0	41.5	1.50	1.20	−5.4
89	09:57:26.987	17.29	2.55	24.01	2.63	24.51	23.03	75.1	34.0	41.6	0.99	0.79	−5.5
90	09:57:32.107	8.22	2.64	24.33	2.68	24.57	10.98	75.1	34.0	41.7	0.47	0.38	−5.5
IMPACT	09:57:36.756												

Table 2. (Cont'd)
c. Camera P_1

Photo number	GMT of frame exposure Feb. 20, 1965	Spacecraft			Photograph (central reticle)						Scale, km		Deviation north, deg
		Altitude, km	Latitude, deg	Longitude, deg	Latitude, deg	Longitude, deg	Slant range, km	Incidence angle, deg	Phase angle, deg	Emission angle, deg	E-W	N-S	
1	09:46:17.339	1247.59	−4.41	−0.24	−4.70	7.97	1289.23	58.3	39.1	19.3	38.39	33.69	−1.6
2	09:49:43.141	868.44	−3.00	4.77	−2.39	13.24	923.64	63.6	39.1	24.6	28.50	24.20	−2.1
3	09:51:12.182	703.56	−2.24	7.41	−1.39	15.51	761.72	65.9	39.1	26.9	23.94	19.99	−2.5
4	09:55:35.105	218.71	0.77	17.83	1.48	21.97	256.89	72.5	39.1	33.8	8.61	6.81	−4.1
5	09:56:26.346	125.79	1.54	20.50	2.01	23.13	151.15	73.7	39.1	35.0	5.13	4.01	−4.5
6	09:57:24.307	22.04	2.50	23.85	2.60	24.37	27.28	74.9	39.1	36.4	0.94	0.73	−4.9
7	09:57:25.147	20.55	2.51	23.90	2.60	24.38	25.45	74.9	39.1	36.4	0.88	0.68	−4.9
8	09:57:25.987	19.06	2.53	23.95	2.61	24.40	23.62	75.0	39.1	36.4	0.81	0.63	−4.9
9	09:57:26.827	17.57	2.54	24.00	2.62	24.42	21.78	75.0	39.1	36.4	0.75	0.58	−4.9
10	09:57:27.667	16.08	2.56	24.05	2.63	24.44	19.94	75.0	39.1	36.4	0.69	0.53	−4.9
11	09:57:28.507	14.60	2.57	24.11	2.64	24.45	18.11	75.0	39.1	36.5	0.62	0.48	−4.9
12	09:57:29.347	13.11	2.59	24.16	2.65	24.47	16.27	75.0	39.1	36.5	0.56	0.43	−4.9
13	09:57:30.187	11.62	2.60	24.21	2.66	24.49	14.43	75.0	39.1	36.5	0.50	0.38	−4.9
14	09:57:31.027	10.13	2.62	24.26	2.66	24.50	12.59	75.1	39.1	36.5	0.43	0.34	−4.9
15	09:57:31.867	8.64	2.63	24.31	2.67	24.52	10.74	75.1	39.1	36.5	0.37	0.29	−4.9
16	09:57:32.707	7.16	2.65	24.37	2.68	24.54	8.90	75.1	39.1	36.5	0.31	0.24	−4.9
17	09:57:33.547	5.67	2.66	24.42	2.69	24.56	7.06	75.1	39.1	36.6	0.24	0.19	−4.9
18	09:57:34.387	4.19	2.68	24.47	2.70	24.57	5.21	75.1	39.1	36.6	0.18	0.14	−4.9
19	09:57:35.227	2.70	2.69	24.52	2.71	24.59	3.36	75.2	39.1	36.6	0.12	0.09	−4.9
20	09:57:36.067	1.22	2.71	24.58	2.71	24.61	1.52	75.2	39.1	36.6	0.05	0.04	−4.9
IMPACT	09:57:36.756												

Table 2. (Cont'd)
d. Camera P_2

Photo number	GMT of frame exposure Feb. 20, 1965	Spacecraft			Photograph (central reticle)						Scale, km		Deviation north, deg
		Altitude, km	Latitude, deg	Longitude, deg	Latitude, deg	Longitude, deg	Slant range, km	Incidence angle, deg	Phase angle, deg	Emission angle, deg	E-W	N-S	
1	09:46:17.739	1246.85	−4.40	−0.23	−3.92	7.97	1288.52	58.3	39.1	19.3	50.03	34.27	−1.9
2	09:49:43.541	867.70	−2.99	4.78	−1.83	13.24	923.60	63.6	39.1	24.7	37.17	24.67	−2.4
3	09:51:12.582	702.82	−2.24	7.43	−0.93	15.52	761.82	65.9	39.2	27.1	31.24	20.41	−2.7
4	09:55:35.505	217.98	0.78	17.85	1.64	21.98	256.63	72.5	39.2	34.0	11.22	6.95	−4.2
5	09:56:26.746	125.07	1.55	20.52	2.10	23.14	150.68	73.7	39.2	35.3	6.68	4.09	−4.5
6	09:57:24.707	21.33	2.51	23.87	2.62	24.38	26.48	74.9	39.1	36.6	1.19	0.72	−4.9
7	09:57:25.547	19.84	2.52	23.92	2.62	24.39	24.64	75.0	39.1	36.6	1.11	0.67	−4.9
8	09:57:26.387	18.35	2.54	23.98	2.63	24.41	22.80	75.0	39.1	36.6	1.03	0.62	−4.9
9	09:57:27.227	16.86	2.55	24.03	2.64	24.43	20.96	75.0	39.1	36.6	0.94	0.57	−4.9
10	09:57:28.067	15.38	2.57	24.08	2.65	24.44	19.12	75.0	39.1	36.7	0.86	0.52	−4.9
11	09:57:28.907	13.89	2.58	24.13	2.65	24.46	17.28	75.0	39.1	36.7	0.78	0.47	−4.9
12	09:57:29.747	12.40	2.60	24.18	2.66	24.48	15.43	75.0	39.1	36.7	0.70	0.42	−4.9
13	09:57:30.587	10.91	2.61	24.24	2.67	24.50	13.59	75.1	39.1	36.7	0.61	0.37	−4.9
14	09:57:31.427	9.42	2.63	24.29	2.67	24.51	11.74	75.1	39.1	36.7	0.53	0.32	−4.9
15	09:57:32.267	7.94	2.64	24.34	2.68	24.53	9.89	75.1	39.1	36.7	0.45	0.27	−4.9
16	09:57:33.107	6.45	2.66	24.39	2.70	24.55	8.04	75.1	39.1	36.8	0.36	0.22	−4.9
17	09:57:33.947	4.96	2.67	24.44	2.70	24.56	6.19	75.1	39.1	36.8	0.28	0.17	−4.9
18	09:57:34.787	3.48	2.69	24.50	2.70	24.58	4.34	75.1	39.2	36.8	0.20	0.12	−4.9
19	09:57:35.627	1.99	2.70	24.55	2.71	24.60	2.49	75.2	39.2	36.8	0.11	0.07	−4.9
20	09:57:36.467	0.51	2.72	24.60	2.72	24.61	0.64	75.2	39.2	36.8	0.03	0.02	−4.9
IMPACT	09:57:36.756												

Table 2. (Cont'd)
e. Camera P_3

Photo number	GMT of frame exposure Feb. 20, 1965	Spacecraft			Photograph (central reticle)						Scale, km		Deviation north, deg
		Altitude, km	Latitude, deg	Longitude, deg	Latitude, deg	Longitude, deg	Slant range, km	Incidence angle, deg	Phase angle, deg	Emission angle, deg	E-W	N-S	
1	09:46:17.539	1247.22	−4.40	−0.24	−4.66	8.78	1297.25	59.1	38.1	21.1	113.24	107.28	−1.6
2	09:49:43.341	868.07	−2.99	4.77	−2.36	13.84	931.06	64.2	38.1	26.2	84.21	77.41	−2.2
3	09:51:12.382	703.19	−2.24	7.42	−1.36	16.02	768.45	66.4	38.1	28.5	70.77	64.10	−2.6
4	09:55:35.305	218.34	0.77	17.84	1.49	22.15	259.58	72.7	38.1	35.0	25.40	21.95	−4.2
5	09:56:26.546	125.43	1.54	20.51	2.02	23.24	152.64	73.8	38.1	36.2	15.13	12.95	−4.6
6	09:57:24.507	21.69	2.50	23.86	2.60	24.39	27.20	74.9	38.1	37.4	2.73	2.32	−5.0
7	09:57:25.347	20.20	2.52	23.91	2.61	24.41	25.34	75.0	38.1	37.4	2.55	2.16	−5.0
8	09:57:26.187	18.71	2.53	23.96	2.62	24.42	23.48	75.0	38.1	37.4	2.36	2.00	−5.0
9	09:57:27.027	17.22	2.55	24.01	2.62	24.44	21.63	75.0	38.1	37.4	2.17	1.84	−5.0
10	09:57:27.867	15.73	2.56	24.07	2.63	24.45	19.76	75.0	38.1	37.5	1.99	1.68	−5.0
11	09:57:28.707	14.24	2.58	24.12	2.64	24.47	17.90	75.0	38.1	37.5	1.80	1.52	−5.0
12	09:57:29.547	12.75	2.59	24.17	2.65	24.49	16.04	75.0	38.1	37.5	1.61	1.37	−5.0
13	09:57:30.387	11.26	2.61	24.22	2.66	24.50	14.17	75.1	38.1	37.5	1.43	1.21	−5.0
14	09:57:31.227	9.78	2.62	24.27	2.67	24.52	12.31	75.1	38.1	37.5	1.24	1.05	−5.0
15	09:57:32.067	8.29	2.64	24.33	2.67	24.53	10.44	75.1	38.1	37.5	1.05	0.89	−5.0
16	09:57:32.907	6.80	2.65	24.38	2.68	24.55	8.57	75.1	38.1	37.6	0.86	0.73	−5.0
17	09:57:33.747	5.32	2.67	24.43	2.69	24.56	6.70	75.1	38.1	37.6	0.68	0.57	−5.0
18	09:57:34.587	3.83	2.68	24.48	2.70	24.58	4.83	75.1	38.1	37.6	0.49	0.41	−5.0
19	09:57:35.427	2.35	2.70	24.54	2.71	24.60	2.96	75.2	38.1	37.6	0.30	0.25	−5.0
20	09:57:36.267	0.86	2.71	24.59	2.72	24.61	1.09	75.2	38.1	37.6	0.11	0.09	−5.1
IMPACT	09:57:36.756												

Table 2. (Cont'd)
f. Camera P_4

Photo number	GMT of frame exposure Feb. 20, 1965	Spacecraft			Photograph (central reticle)						Scale, km		Deviation north, deg
		Altitude, km	Latitude, deg	Longitude, deg	Latitude, deg	Longitude, deg	Slant range, km	Incidence angle, deg	Phase angle, deg	Emission angle, deg	E-W	N-S	
1	09:46:17.939	1246.49	−4.40	−0.23	−3.91	8.82	1296.97	59.2	38.1	21.2	112.71	106.99	−1.8
2	09:49:43.741	867.33	−2.99	4.78	−1.82	13.88	931.39	64.2	38.1	26.4	83.89	77.35	−2.4
3	09:51:12.782	702.45	−2.23	7.43	−0.91	16.05	768.88	66.5	38.1	28.7	70.53	64.10	−2.8
4	09:55:35.705	217.61	0.78	17.86	1.64	22.18	259.46	72.7	38.1	35.3	25.31	21.95	−4.3
5	09:56:26.946	124.71	1.55	20.53	2.11	23.26	152.24	73.8	38.1	36.4	15.04	12.92	−4.7
6	09:57:24.907	20.98	2.51	23.88	2.62	24.40	26.40	75.0	38.1	37.6	2.65	2.25	−5.0
7	09:57:25.747	19.49	2.53	23.94	2.63	24.42	24.54	75.0	38.1	37.7	2.46	2.09	−5.0
8	09:57:26.587	18.00	2.54	23.99	2.63	24.43	22.67	75.0	38.1	37.7	2.27	1.93	−5.0
9	09:57:27.427	16.51	2.55	24.04	2.64	24.45	20.81	75.0	38.1	37.7	2.09	1.77	−5.0
10	09:57:28.267	15.02	2.57	24.09	2.65	24.46	18.94	75.0	38.1	37.7	1.90	1.61	−5.0
11	09:57:29.107	13.53	2.58	24.14	2.65	24.48	17.07	75.0	38.1	37.7	1.71	1.45	−5.0
12	09:57:29.947	12.04	2.60	24.20	2.66	24.49	15.20	75.1	38.1	37.7	1.52	1.30	−5.0
13	09:57:30.787	10.56	2.61	24.25	2.67	24.51	13.33	75.1	38.1	37.8	1.34	1.14	−5.0
14	09:57:31.627	9.07	2.63	24.30	2.68	24.53	11.46	75.1	38.1	37.8	1.15	0.98	−5.0
15	09:57:32.467	7.58	2.64	24.35	2.68	24.54	9.58	75.1	38.1	37.8	0.96	0.82	−5.0
16	09:57:33.307	6.10	2.66	24.40	2.69	24.56	7.71	75.1	38.1	37.8	0.77	0.66	−5.0
17	09:57:34.147	4.61	2.67	24.46	2.70	24.57	5.83	75.1	38.1	37.8	0.59	0.50	−5.1
18	09:57:34.987	3.13	2.69	24.51	2.71	24.59	3.96	75.1	38.1	37.8	0.40	0.34	−5.1
19	09:57:35.827	1.64	2.70	24.56	2.71	24.60	2.08	75.2	38.1	37.9	0.21	0.18	−5.1
20	09:57:36.667	0.16	2.72	24.61	2.72	24.62	0.20	75.2	38.1	37.9	0.02	0.02	−5.1
IMPACT	09:57:36.756												

REFERENCES

1. Rindfleisch, T. C., and Willingham, D. E., *Figure of Merit as a Measure of Picture Resolution,* Technical Report No. 32-666, Jet Propulsion Laboratory, Pasadena, California, September 1, 1965.

2. Kirhofer, W. E., *Television Constraints and Digital Computer Program,* Technical Report No. 32-667, Jet Propulsion Laboratory, Pasadena, California (to be published).

3. Sytinskaya, N. N., and Sharonov, V. V., "Study of the Reflecting Power of the Moon's Surface," *Uchenye Zapiski Lgu,* No. 153 (1952), p. 114. (Translated by Space Technology Laboratories, Inc., Los Angeles, California, as STL-TR-61-5110-23, May 1961.)

4. Willingham, D. E., *The Lunar Reflectivity Model for Ranger Block III Analysis,* Technical Report No. 32-664, Jet Propulsion Laboratory, Pasadena, California, November 2, 1964.

5. Smith, G. M., and Willingham, D. E., *Ranger Photometric Calibration,* Technical Report No. 32-665, Jet Propulsion Laboratory, Pasadena, California August 15, 1965.